0026-895X/90/050667-07$03.00/0

MOLECULAR PHARMACOLOGY, 38:667-673

Identification and Properties of Voltage-Sensitive Sodium Channels in Smooth Muscle Cells from Pregnant Rat Myometrium

CÉCILE MARTIN, SERGE ARNAUDEAU, KHADIJA JMARI, LALA RAKOTOARISOA, IRÈNE SAYET, CATHERINE DACQUET, CHANTAL MIRONNEAU, and JEAN MIRONNEAU

Laboratoire de Physiologie Cellulaire et Pharmacologie Moléculaire, INSERM CJF 88-13, Université de Bordeaux II, 33076 Bordeaux, France

Received February 28; 1990; Accepted August 6; 1990

SUMMARY

Saturable high and low affinity binding sites for [^{3}H]saxitoxin were identified in myometrial membranes of pregnant rats, with dissociation constants of 0.53 and 27 nM, respectively. The maximal binding capacity of the low affinity binding sites was about 10 times higher than that of the high affinity binding sites. The dissociation constants obtained from association and dissociation kinetics of [^{3}H]saxitoxin were similar to those obtained from equilibrium binding. Saxitoxin and tetrodotoxin specifically displaced [^{3}H]saxitoxin binding at both types of sites. Isradipine (1–10 μM) and amiloride (50–100 μM) were without effect on the binding of [^{3}H]saxitoxin. At high concentrations (10–100 μM), veratridine induced a partial inhibition of [^{3}H]saxitoxin binding. In dispersed myometrial cells, [^{3}H]saxitoxin binding revealed the presence of both high and low affinity binding sites, with K_D values similar to those obtained in myometrial membranes. Sodium currents were studied in both freshly dispersed and cultured myometrial cells in the presence of veratridine (100 μM), using the whole-cell patch-clamp technique. Steady state inactivation curves indicated that sodium channels were available at negative membrane potentials (between −110 and −40 mV). Isradipine (1–10 μM) and amiloride (50–100 μM) were without effect on the sodium current. Applications of saxitoxin or tetrodotoxin inhibited the amplitude of the sodium current in a concentration-dependent manner. The concentrations of saxitoxin and tetrodotoxin producing half-maximal inhibition were 1.4 and 8.8 nM, respectively. Although the IC_{50} values for saxitoxin and tetrodotoxin found from electrophysiological experiments are not identical to the equilibrium dissociation constants for the high and low affinity sites found from binding experiments, these results suggested that binding of the neurotoxins to the high affinity sites may be involved in their inhibitory effects on sodium channels. Furthermore, low affinity binding sites may be associated with a nonfunctional subtype of sodium channels in myometrial cells.

Voltage-gated sodium channels are transmembrane proteins that mediate the early increase in sodium flux underlying the initial depolarization of the action potential in many excitable cells (1). Characterization of sodium channels has been advanced through the use of the selective sodium channel blockers STX and TTX. It is now clear that mammalian sodium channels are encoded by a multigene family (2) and show different functional properties in different tissues. The most widely known difference is that TTX-sensitive sodium channels in nerve and skeletal muscle are blocked by nanomolar concentrations of the neurotoxins (3, 4), whereas TTX-resistant sodium channels in cardiac muscle and noninnervated skeletal muscle require micromolar concentrations of the neurotoxins to block them (5, 6).

This work was supported by grants from Etablissement Public Régional d'Aquitaine, Ministère de la Recherche et de la Technologie, Fondation pour la Recherche Médicale and Association Française contre les Myopathies, France.

In myometrial smooth muscle cells, sodium-dependent action potentials have been first reported using the microelectrode technique (7). More recently, TTX-sensitive sodium currents have been described in freshly dissociated cells from pulmonary artery (8) and myometrium of pregnant rats (9). However, no complete biochemical analysis has been made for the presence of sodium channels in smooth muscle using radioligand experiments. In the present report, we characterize the [^{3}H]STX binding sites in both myometrial membranes and intact cells from pregnant rat uterus. We demonstrate that high and low affinity sites for STX and TTX coexist in the membrane of myometrial cells and that the binding of the neurotoxins to the high affinity sites may be involved in their inhibitory effects on sodium channels.

Materials and Methods

Membrane preparation. The uterus was removed from pregnant Wistar rats (18–20 days of gestation). Endometrium was scrapped off

ABBREVIATIONS: STX, saxitoxin; TTX, tetrodotoxin; HEPES, *N*-2-hydroxyethylpiperazine-*N'*-2-ethanesulfonic acid; QNB, quinuclidinylbenzilate; EGTA, ethylene glycol bis-(β-aminoethyl ether)-*N,N,N',N'-tetraacetic acid.*

and myometrial membranes were prepared in the presence of 1 mM iodoacetamide and 0.1 mM phenylmethylsulfonyl fluoride (10). Proteins were assayed according to the method of Bradford (11), with γ-globulins as standard.

Single-cell isolation procedure. The enzymatic dispersion procedure for isolating single myometrial cells and the method of short term primary culture were identical to those described previously (12).

[^{3}H]STX binding. In the binding assay using myometrial membranes, membrane proteins (0.05–0.25 mg/ml) were incubated with [^{3}H]STX (63 Ci/mmol) in 1 ml of 20 mM HEPES buffer (pH 7.4), 0.01% bovine serum albumin, at 25° for 45 min. Bound and free radioligand were separated by rapid filtration through Whatman GF/C glass fiber filters. The filters were rinsed twice with 8 ml of ice-cold 0.1 M Tris buffer (pH 7.4), and radioactivity bound to them was measured in a liquid scintillation counter at an efficiency of approximately 55%. Nonspecific binding was assessed in the presence of a large excess of unlabeled STX (2–10 μM). Analysis of low affinity [^{3}H]STX binding was done with a 1:12 ratio of [^{3}H]STX to unlabeled STX, so that concentrations of STX up to 60 nM could be assayed for binding. Radioligand binding data were analyzed using the nonlinear least-squares LIGAND program for multiple binding sites (13), with the assistance of an IBM computer.

In the binding assay using intact cells, the cell suspension was incubated at 30° for 45 min in 1 ml of a physiological solution containing (in mM): choline chloride, 130; KCl, 5.6; $CaCl_2$, 1.8; $MgCl_2$, 0.24; HEPES, 10; and glucose, 11; pH 7.4; with increasing concentrations of [^{3}H]STX. The cell number was 4–5 × 10^4 cells/ml. The binding was halted by a rapid filtration of the cell suspension through Whatman GF/C glass fiber filters. The filters were washed twice with 8 ml of ice-cold physiological solution. Nonspecific binding was defined as the amount of radioligand bound in the presence of 2–10 μM unlabeled STX and was subtracted from the total binding. The membrane potential of freshly dispersed myometrial cells measured with intracellular microelectrodes was estimated to be −45.4 ± 5.5 mV (n = 19). Because this value was close to the resting potential of myometrial cells, these dispersed cells served as the intact cells.

Other binding assays. Myometrial membranes were also characterized by [^{3}H]QNB and (+)-[^{3}H]isradipine. Temperature and incubation time were 25° and 60 min, respectively. Nonspecific binding was defined with 2 μM atropine for [^{3}H]QNB binding and with 2 μM nitrendipine for (+)-[^{3}H]isradipine binding.

Patch-clamp recordings. Membrane currents were recorded using the whole-cell patch-clamp technique in single myometrial cells, freshly dissociated or maintained in short term primary culture for up to 2 days (14). The pipette solution contained (in mM): CsCl, 110; NaCl, 30; Na_2ATP, 5; $MgCl_2$, 5; EGTA, 10; and HEPES, 10 (pH 7.3 with CsOH). The bath solution contained (in mM): NaCl, 130; CsCl, 5.6; $BaCl_2$, 5; $MgCl_2$, 1.24; glucose, 11; and Tris, 8.3 (pH 7.4 with HCl). The bath solution was maintained at 30 ± 0.5°. In selectivity experiments, external NaCl was substituted by Tris-HCl and internal CsCl was substituted by NaCl. The electrophysiological data were filtered with an eight-pole Bessel filter at 1 kHz and analyzed with an IBM PS2 microcomputer.

Chemicals. [^{3}H]STX (63 Ci/mmol), (+)-[^{3}H]isradipine (83 Ci/mmol), and [^{3}H]QNB (46 Ci/mmol) were obtained from Amersham (France). Atropine, iodoacetamide, phenylmethylsulfonyl fluoride, bovine serum albumin, veratridine, and amiloride were obtained from Sigma and the protein assay kit from Bio-Rad (Munich, FRG). Unlabeled TTX and STX were obtained from Calbiochem. (+)-Isradipine was a gift from Sandoz (Basel, Switzerland).

Data are presented as means ± standard errors, with n equal to the sample size.

Results

Equilibrium binding of [^{3}H]STX to myometrial membranes. The specific binding of [^{3}H]STX to its receptor was proportional to the concentration of myometrial membranes from 0.05 mg of protein/ml to 0.40 mg of protein/ml. This proportionality was also found by using different [^{3}H]STX concentrations between 0.07 and 15 nM. The saturability of [^{3}H]STX binding to myometrial membranes with increasing concentrations of tritiated ligand is shown in Fig. 1 (*inset*). The Scatchard plot of the specific binding component indicates the existence of both high and low affinity binding sites. The dissociation constants (K_D) and maximal binding capacities (B_{max}) were (K_D = 0.53 ± 0.11 nM and B_{max} = 39 ± 5 fmol/mg of protein for the high affinity site and K_D = 27 ± 6 nM and B_{max} = 350 ± 45 fmol/mg of protein for the low affinity binding site (n = 6). Heat treatment (65°, 20 min) or trypsin treatment (0.1 mg/ml) of myometrial membranes resulted in a large inhibition of binding (80–90%) to the two families of sites.

High affinity binding site for [^{3}H]STX in myometrial membranes. The properties of the high affinity [^{3}H]STX site were examined using 0.4 nM [^{3}H]STX. Under these conditions, about 80% of the signal originated from binding to the high affinity binding site and 20% from binding to the low affinity binding site. Typical kinetics of association of [^{3}H]STX are presented in Fig. 2A. Fig. 2A, *inset* shows that the semilogarithmic representation of the data is linear, as expected for a pseudo-first-order reaction. The experimental rate constant measured in association experiments was k_{obs} = 0.099 ± 0.010 min^{-1} (n = 4). Furthermore, $K_{obs} = k_1$ ([^{3}H]STX) + k_{-1}, in which k_1 and k_{-1} represent, respectively, the rate constants of association and dissociation of the [^{3}H]STX-receptor complex. Fig. 2B shows that [^{3}H]STX bound to myometrial membranes can be displaced by unlabeled STX. Because of the large excess of unlabeled STX (2 μM), the reassociation of [^{3}H]STX with the receptor was prevented, and then the dissociation was a first-order reaction. As expected, the semilogarithmic representation of the dissociation data was linear, as shown in Fig. 2B, *inset*, and gave a rate constant for dissociation (k_{-1}) of 0.050 ± 0.005 min^{-1} (n = 4). The calculated value of k_1 was 0.122 ±

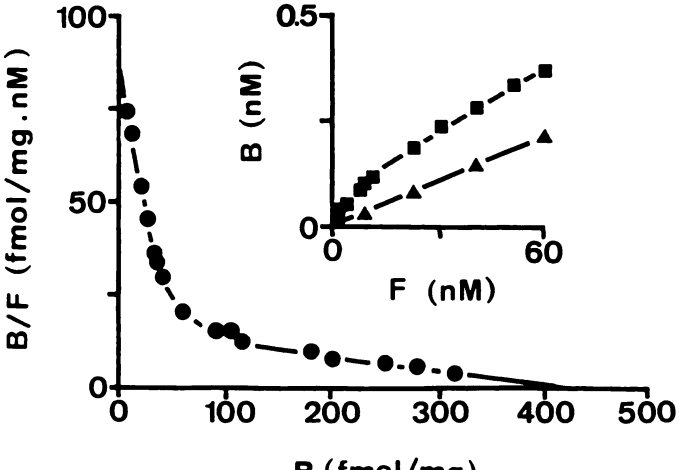

Fig. 1. Specific binding of [^{3}H]STX to myometrial membranes. *Inset*, saturation binding experiments were carried out by incubating myometrial smooth muscle membranes (0.25 mg/ml protein) with increasing concentrations of [^{3}H]STX for 45 min at 25° ■, Total binding; ▲, nonspecific binding, defined with 10 μM STX. *Main panel*, Scatchard plot of the specific binding, indicating the existence of both high and low affinity binding sites for STX. Duplicate estimates were used for each point; similar estimates were obtained from six separate experiments. *B/F*, bound/free. Saturation curves were analyzed with the assistance of an IBM computer, using the nonlinear least-squares LIGAND program (13).

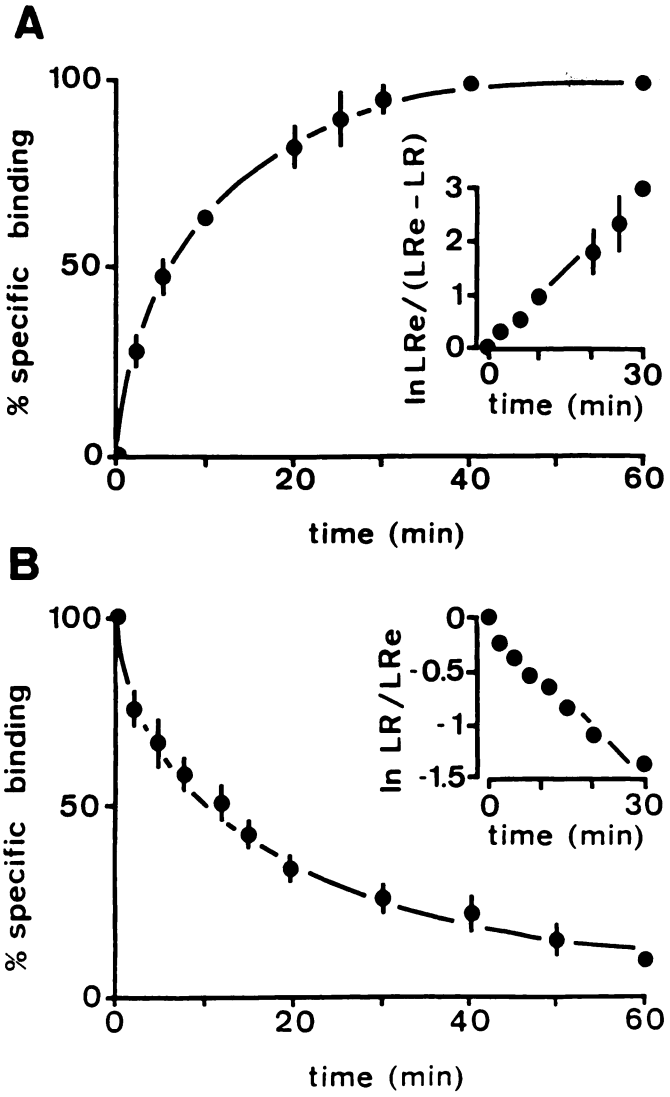

Fig. 2. Association and dissociation kinetics for the specific high affinity binding of [^{3}H]STX to myometrial membranes. A, Association was initiated by addition of [^{3}H]STX (final concentration, 0.4 nM) to an assay mixture containing 0.2 mg/ml membranes. At the indicated times, an aliquot of the mixture was withdrawn, and the association was terminated by rapid filtration. Nonspecific binding, determined with 2 μM STX, was constant. *Inset*, pseudo-first-order representation of the data. LR_e, concentration of [^{3}H]STX-receptor complex at equilibrium; *LR*, concentration of the complex at time *t*. B, Dissociation of specific binding. After equilibrium had been reached, dissociation was monitored after addition of 2 μM unlabeled STX. *Inset*, first-order representation of binding. Each *point* represents the mean response in three experiments, with the standard error shown by *vertical lines*.

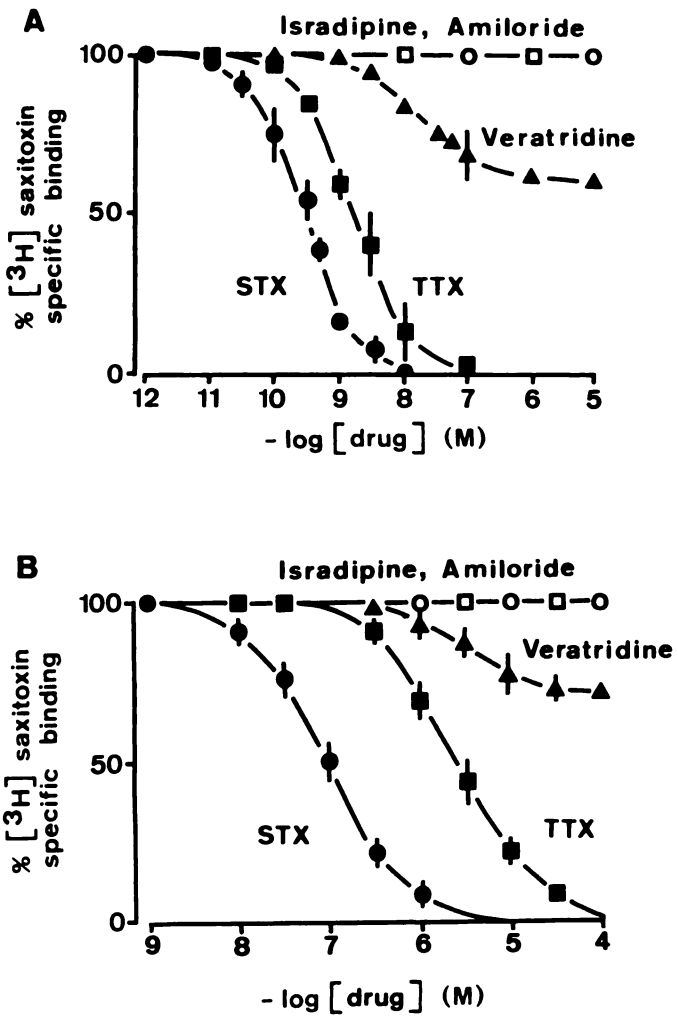

Fig. 3. Effects of STX, TTX, veratridine, (+)-israpidine, and amiloride on [^{3}H]STX binding to myometrial membranes. A, High affinity binding sites. Membranes (0.15 mg/ml protein) were incubated for 45 min in the presence of 0.4 nM [^{3}H]STX and varying concentrations of unlabeled STX (●), TTX (■), veratridine (▲), (+)-isradipine (○), and amiloride (□). B, Low affinity binding sites. Membranes (0.20 mg of protein/ml) were incubated with 15 nM [^{3}H]STX (5 Ci/mmol) and varying concentrations of unlabeled STX (●), TTX (■), veratridine (▲), (+)-isradipine (○), and amiloride (□). Results are expressed as a percentage of the specific binding obtained in the absence of unlabeled drugs. Each *point* represents the mean response in three or four experiments, with the standard error shown by *vertical lines*.

0.030 nM^{-1} min^{-1} and the dissociation constant from kinetic data ($K_D = k_{-1}/k_1$) was estimated to be 0.4–0.5 nM. This value is in good agreement with the value of K_D obtained from equilibrium binding measurements (Fig. 1).

Increasing concentrations of unlabeled STX or TTX inhibited the [^{3}H]STX binding (Fig. 3A). The inhibition constant values (K_i) for STX and TTX, calculated with the equation of Cheng and Prussoff (15), were 0.18 ± 0.02 and 0.94 ± 0.04 nM, respectively (n = 4). The Hill coefficients were close to 1, indicating that the drugs bound to a single binding site. In contrast, veratridine inhibited [^{3}H]STX binding by 35 ± 4% (n = 4). The concentration producing half-maximal inhibition and the slope factor of the inhibition curve were calculated to be 25 ± 3 nM and 0.58 ± 0.08, respectively (n = 4). Calcium entry blockers such as (+)-isradipine were without effect on [^{3}H]STX binding at concentrations (1 nM to 1 μM) that blocked voltage-dependent calcium channels (14). Amiloride, a blocker of sodium channels in epithelia (16), did not alter [^{3}H]STX binding to myometrial membranes, even at concentrations as high as 100 μM.

Low affinity binding site for [^{3}H]STX in myometrial membranes. The properties of the low affinity STX site were examined using 15 nM [^{3}H]STX. Under these conditions, about 80% of the total bound ligand was associated with the low affinity binding site. The rate constants for association and dissociation were 0.00233 ± 0.00011 nM^{-1} min^{-1} and 0.070 ± 0.003 min^{-1}, respectively (n = 4). The calculated dissociation constant from kinetic data was estimated to be about 30 nM, a value similar to that obtained from equilibrium binding exper-

iments. As shown in Fig. 3B, increasing concentrations of unlabeled neurotoxins inhibited [^{3}H]STX binding to the low affinity binding site. The inhibition constant values (K_i) for STX and TTX were 55 ± 9 nM (n = 4) and 1.2 ± 0.4 μM (n = 4), respectively. The Hill coefficients were close to 1, suggesting that the neurotoxins bound to a single binding site. In contrast, veratridine inhibited [^{3}H]STX binding by 30 ± 5% (n = 4). The IC_{50} and the slope factor of the inhibition curve were 5.5 ± 0.5 μM and 0.55 ± 0.05, respectively (n = 4). Amiloride as well as (+)-isradipine were without effect on [^{3}H]STX binding to the low affinity site (n = 3).

Other binding assays in myometrial membranes. Specific high affinity binding sites for [^{3}H]QNB and (+)-[^{3}H] isradipine were present in myometrium membranes. The dissociation constants of [^{3}H]QNB (K_D = 0.035 ± 0.010 nM, n = 4) and (+)-[^{3}H]isradipine (K_D = 0.090 ± 0.010 nM, n = 6) were lower than that of [^{3}H]STX (K_D = 0.53 ± 0.11 nM, n = 6). In contrast, the density of muscarinic receptors (B_{max} = 320 ± 50 fmol/mg of protein, n = 4) was higher than the density of dihydropyridine (B_{max} = 95 ± 5 fmol/mg of protein, n = 6) and saxitoxin (B_{max} = 39 ± 5 fmol/mg of protein, n = 6) receptors.

Equilibrium binding of [^{3}H]STX to isolated myometrial cells. Binding of [^{3}H]STX to dispersed myometrial cells was carried out in order to verify that both high and low affinity binding sites were present in the plasma membrane. Specific binding of [^{3}H]STX increased linearly with cell density up to 10^5 cells/ml. The following binding experiments were carried out in the linear range, 4–5 × 10^4 cells/ml, using either 0.4 or 15 nM [^{3}H]STX. In each case, the specific binding was saturable and Scatchard analysis resulted in a linear plot. The K_D and B_{max} values were 0.38 ± 0.05 nM and 18 ± 2.5 fmol/4 × 10^4 cells, respectively, for the high affinity site (n = 6) and 21 ± 5 nM and 172 ± 21 fmol/4 × 10^4 cells for the low affinity site (n = 3). The dissociation constant values obtained from dispersed myometrial cells are clearly similar to those obtained from myometrial membranes, indicating that both affinity binding sites for [^{3}H]STX are located in the plasma membrane of smooth muscle cells.

Patch-clamp identification of the veratridine-activated current. Recent studies have shown the existence of fast sodium currents in smooth muscle cells including myometrium (8, 9). Because the fast sodium current peaks within 2–3 msec, capacitive transients have to be reduced by using small cells and electrodes with a relatively low resistance. In most cases, the first 1–3 msec are not properly clamped and the peak current amplitude may be underestimated, especially for the high depolarizing pulses. Neurotoxins such as veratridine and sea anemone toxins have been shown to reveal the voltage-dependent sodium current by stabilizing an open form of the sodium channel (1, 7). When 100 μM veratridine was applied in the bath solution to a voltage-clamped freshly dissociated myometrial cell, the inward barium current elicited by a positive voltage pulse was progressively inhibited within 2–3 min. After the pulse, there was a standing inward tail current representing a population of veratridine-modified channels that did not close at −90 mV (Fig. 4A). The tail current decayed to zero within several seconds. In the continuous presence of external veratridine, the tail current was recorded without a noticeable variation in amplitude for 5–10 min. Similar tail currents activated by veratridine were obtained in cells maintained in short term primary culture for up to 2 days. In the following

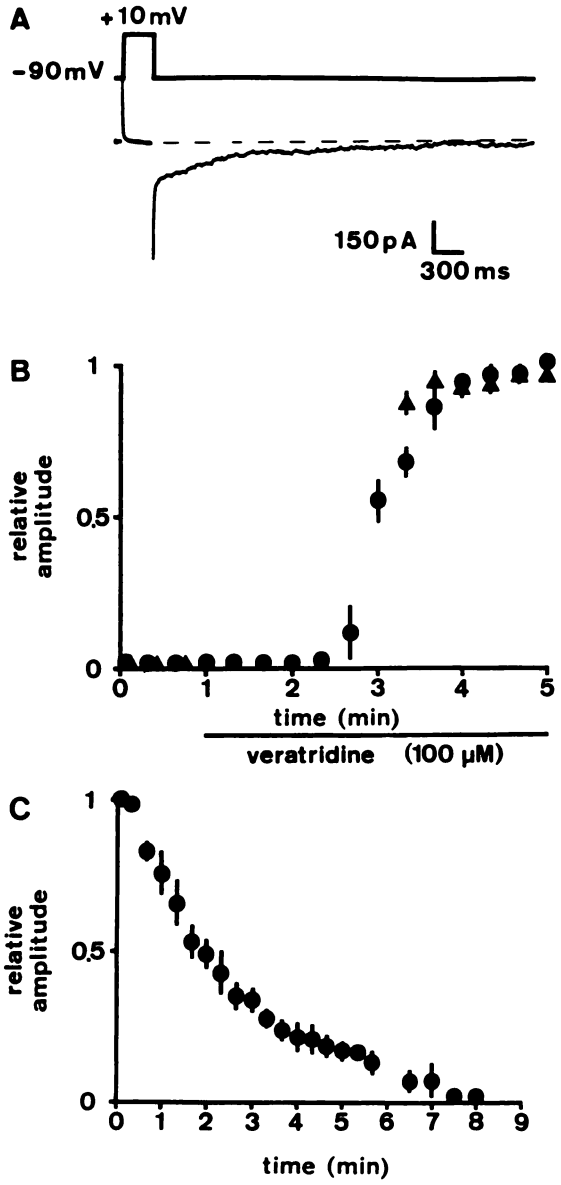

Fig. 4. Veratridine-activated inward currents in single cells isolated from pregnant rat myometrium. A, Membrane current obtained in a freshly isolated myometrial cell superfused in the presence of 100 μM veratridine for 4 min. The cell was depolarized from −90 mV to +10 mV for 300 msec. A long lasting inward tail current appeared upon return to −90 mV, whereas the inward current during the depolarizing pulse was masked by leakage current. B, Effects of veratridine (100 μM) with (●) and without (▲) repetitive applications of command pulses (20-sec intervals). The membrane was stepped to 0 mV (300-msec duration) from a holding potential of −90 mV. Each *point* is the mean response of three to seven experiments, with the standard error shown by *vertical lines*. Steady state effect of veratridine was obtained within 3 min. C, after removal of veratridine, the inward tail current progressively disappeared. After 8 min of washing out, there was no tail current. Currents are expressed as a fraction of their maximal values.

experiments, veratridine-activated currents were recorded in freshly dissociated cells as well as in cultured myometrial cells.

Previous papers have studied in detail the state dependence of sodium channel modification induced by veratridine, using whole-cell and single-channel recordings in muscle and nerve cells (17–19). In further experiments we examined whether the action of veratridine depended on the number of command pulses applied (Fig. 4B). Command pulses (300-msec duration,

20-sec intervals) were used to step membrane potential from a holding potential of −90 mV to 0 mV. When such pulses were applied for 1 min, there was no tail current recorded after repolarization to −90 mV. Veratridine (100 μM) was then added to the bath solution and the pattern of command pulses was either maintained (Fig. 4B, *circles*) or recommenced after a 2.3-min rest period (Fig. 4B, *triangles*). In the presence of veratridine, the first post-rest peak tail current represented 90% of the maximal tail current at the end of the maintained pulse train. After removal of veratridine, the inward tail current was progressively reduced and completely disappeared after 7.5 min of wash-out (Fig. 4C). Our results clearly indicate that the effects of veratridine in myometrial cells do not depend on the frequency or number of stimuli used to promote channel opening.

To determine the minimum pulse duration needed to elicit inward tail current upon repolarization to −90 mV, the duration of the depolarizing pulse was varied from 2 to 300 msec. The results indicate that the tail current is maximal for depolarizing pulses lasting 10 msec and remains unchanged when the duration of depolarizing pulses was increased to 300 msec (not shown).

Ion selectivity of the veratridine-activated current. Fig. 5A (*inset*) shows the determination of the reversal potential of the veratridine-activated current. After an initial depolarization to +5 mV from a holding potential of −90 mV, the duration of which was 300 msec, the cell was repolarized to different test potentials to determine the value of the reversal potential (i.e., when there was no tail current). Plotting the maximal tail current against the test potentials showed that the current-voltage relationship was linear (Fig. 5A). The reversal potential was estimated to be 32 ± 2.5 mV ($n = 5$). This value was close to the sodium equilibrium potential calculated on the basis of the Nernst equation ($E_{Na} = 31$ mV). Reversal potentials were determined when the sodium electrochemical gradient was altered by replacing external or internal sodium. Fig. 5B illustrates the plot of the mean reversal potential (E_{rev}) versus the calculated equilibrium potential for sodium ions (E_{Na}). The experimental points were closely distributed along a straight line with a slope of 1, as expected for a pure sodium conductance. The amplitude of the current appeared to be related only to the extracellular sodium concentration, because it was not affected by removal of external barium. Furthermore, there was no variation of the reversal potential when internal caesium was substituted with *N*-methyl-D-glucamine.

Voltage-gating of the veratridine-activated sodium current. The voltage dependency of the sodium current was examined by studying both activation and inactivation curves. As shown in Fig. 6 (*inset*), peak inward tail current recorded at −90 mV was measured as a function of the membrane potential reached during depolarizing pulses. The inward tail current started to develop at −38 ± 4 mV and it reached a maximal value between +10 and +20 mV ($n = 8$). When the inward tail currents were normalized to the current measured at the most positive membrane potential, the activation curve (Fig. 6) was fitted by a Boltzmann distribution, $I/I_{max} = 1/[1 + \exp(V_m - V_h)/k]$, where V_m is the membrane potential, V_h is the midpotential, and k is the slope factor of the curve. Half-maximal activation was obtained at −15 ± 2 mV ($n = 6$).

Inactivation was characterized by use of the classical two-pulse protocol. The amplitude of the tail current was measured

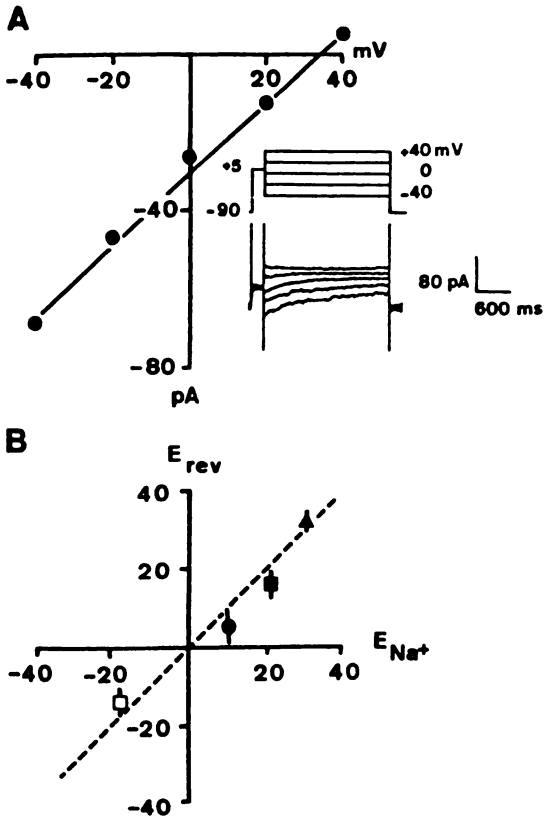

Fig. 5. Ion selectivity of veratridine-activated current. A, Determination of reversal potential of the veratridine-activated current using the two-pulse protocol. *Inset*, after an initial depolarization to +5 mV from a holding potential of −90 mV, the cell was repolarized to different test potentials. The tail current was plotted against the test potentials, and the reversal potential was estimated to be +34 mV. The external sodium concentration was 130 mM and the pipette sodium concentration was 40 mM. Thus, the sodium equilibrium potential calculated on the basis of the Nernst equation was +31 mV. B, Reversal potential (E_{rev}) of the veratridine-activated current as a function of the equilibrium potential for sodium ions (E_{Na}). E_{rev} was determined when the Na electrochemical gradient was altered either by replacing external sodium with Tris (130, 60, and 20 mM Na) or by increasing internal sodium from 40 to 60 mM. Each *point* is the mean response of three to five experiments, with the standard error shown by *vertical lines*. *Dashed line*, reversal potential for a pure sodium conductance.

at −90 mV after application of a test pulse to 10 mV, with a duration of 300 msec. The test pulse was preceded by conditioning pulses of 30-sec duration, to investigate the steady state inactivation process. The variation of the tail current amplitude was taken as an index of inactivation of the sodium current. Relative inactivation (I/I_{max}) was expressed by plotting the tail current against the level of the conditioning pulse (Fig. 6). The amplitude of the tail current versus voltage was fitted by a Boltzmann distribution. The sodium current was fully activatable at −110 mV and presented a half-inactivation potential at −70 ± 3 mV ($n = 5$). Only a very small "steady window current" was found, which did not exceed 5% of the amplitude of the total current and which might not account for the sustained sodium current during depolarizing pulses.

Inhibition of the veratridine-activated sodium current. In Fig. 7, the effects of TTX and STX on the relative amplitude of I_{Na} (I/I_{max}) are shown (holding potential, −90 mV; command pulse, 200 msec to 10 mV). Both STX and TTX applied for 5 min reduced the amplitude of the sodium current

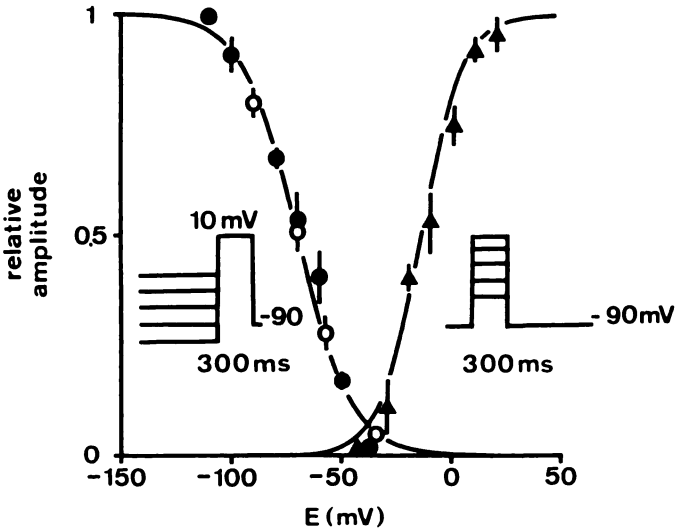

Fig. 6. Steady state activation and inactivation parameters of the veratridine-activated sodium current as a function of the membrane potential. The inactivation (●) and activation (▲) curves, obtained as shown in *insets*, were fitted by an expression of the form $1/[1 + \exp(V_m - V_h)/k]$ with, respectively, the following parameters: $V_h = -14$ mV and $k = -9$ mV for the activation curve and $V_h = -69$ mV and $k = 12$ mV for the inactivation curve. Relative inactivation was also obtained in the presence of 10 nM TTX (○). Each *point* is the mean response of four to eight experiments, with the standard error shown by *vertical lines*.

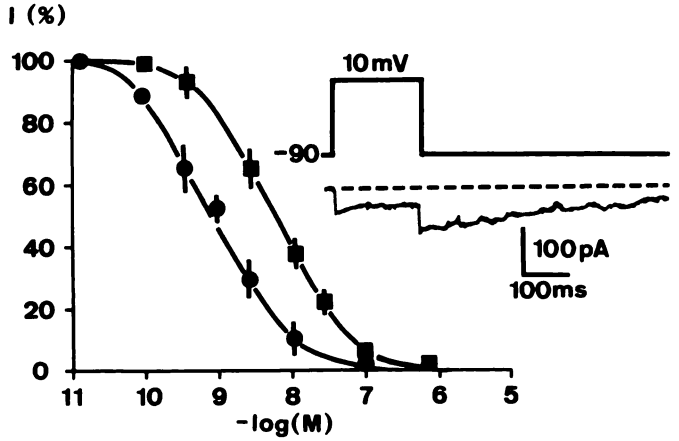

Fig. 7. Concentration-response curves showing the inhibition of the veratridine-activated sodium current, evaluated at 5 min after STX (●) or TTX application (■), with repetitive applications of command pulses (20-sec intervals). Each *point* is the mean response of five experiments, with the standard error shown by *vertical lines*. *Inset*, sustained sodium current obtained by subtracting the currents obtained, in the absence and presence of 1 μM TTX, in response to a depolarizing pulse to +10 mV from a holding potential of −90 mV.

in a concentration-dependent manner. The concentrations of STX and TTX inhibiting 50% of the maximal current (IC_{50}) were estimated to be 1.4 ± 0.3 and 8.8 ± 0.7 nM, respectively ($n = 5$). The slope factor of the concentration-response curve was 0.65 ± 0.01 for STX and 0.63 ± 0.03 for TTX ($n = 5$). Subtraction of the current obtained in the presence and absence of 1 μM TTX revealed that the veratridine-activated sodium current did not inactivate substantially during the depolarizing pulse (Fig. 7, *inset*).

In order to investigate whether TTX bound with a higher affinity to the inactivated state of the sodium channel, a steady state inactivation curve was obtained in the presence of 10 nM TTX. As shown in Fig. 6, no significant differences were found in the presence or absence of TTX. These results indicate clearly that TTX does not inhibit the sodium current in a voltage-dependent manner, as recently shown in myelinated nerve (20).

Isradipine (1 μM) and amiloride (50 μM) were without effect on the veratridine-activated sodium current.

Discussion

In the present study, we have identified high and low affinity receptor binding sites for STX in the membrane of myometrial smooth muscle cells of pregnant rats. The high and low affinity sites are saturable and binding is reversible. The dissociation constants obtained from association and dissociation kinetics of [^{3}H]STX are similar to those obtained from equilibrium binding and competition experiments, suggesting that STX binds to two different receptor sites in myometrial membranes. Both high and low affinity binding sites for [^{3}H]STX have also been identified in intact dispersed myometrial cells, indicating that they are located in the plasma membrane of smooth muscle cells. The dissociation constant values of the high and low affinity binding sites for [^{3}H]STX obtained in myometrial cells are similar to those reported recently in mammalian heart (2). Furthermore, the dissociation constant of the high affinity binding site is nearly identical to that obtained in skeletal muscle (21), synaptosomes (22), and fly head membranes (23).

The complete inhibition induced by TTX of [^{3}H]STX binding to high and low affinity receptors indicates that there are common sites for the two neurotoxins in myometrial membranes. The neurotoxin receptors are different from the receptors for dihydropyridines and amiloride, because both isradipine and amiloride have no effect on [^{3}H]STX binding. In contrast, the partial inhibitory effect of veratridine suggests that binding sites for STX and TTX are distinct from those for veratridine but that they may be allosterically regulated. This observation is in good agreement with the existence of several binding sites for neurotoxins in the sodium channel (1, 24, 25).

The electrophysiological results presented in this paper show that veratridine (100 μM) reveals the sodium current in both freshly dispersed and cultured myometrial cells by stabilizing an open form of sodium channels (1, 26) but inhibits the barium current through voltage-dependent calcium channels (27). Interestingly, the sodium channel remains open during 300-msec depolarizing pulses, and long lasting inward tail currents can be recorded upon repolarizations to −90 mV. In the absence of veratridine, fast sodium currents can be obtained but, because the first 1–3 msec are not properly clamped, the peak current amplitude is not correctly determined.

When sodium channels are opened by a conditioning depolarizing pulse sequence, the effect of veratridine is similar to that obtained in the absence of stimulation. These results suggest that veratridine does not show preferential binding to open or inactivated sodium channels in myometrial cells. Our conclusions that veratridine may bind to resting sodium channels are in good agreement with previous data of Ulbricht (28) in nerve but differ from those of Sutro (17) and Rando (19) in muscle. More detailed experiments are needed to clearly establish the mechanism of action of veratridine on sodium channels in smooth muscle cells.

The veratridine-activated sodium current is selectively blocked by STX and TTX. It is also possible that veratridine

inhibits, in part, the sodium current, because veratridine displaces about 30% of [^{3}H]STX binding. Blockade of sodium channels by STX and TTX is not affected by the membrane potential, because increasing the number of inactivated sodium channels at depolarized holding potentials has no further effect on the neurotoxin-induced inhibition. This observation is supported by the fact that the dissociation constant for the high affinity [^{3}H]STX binding obtained in normally polarized intact myometrial cells (0.38 nM) is similar to that obtained in myometrial membranes (0.53 nM), which are, of course, depolarized. Furthermore, the apparent dissociation constant of STX measured by electrophysiology (1.4 nM) can be considered close to the K_D of [^{3}H]STX for the high affinity membrane receptors. Our data suggest that the high and low affinity sites for STX identified by binding experiments could reflect the existence of two different subtypes of STX-sensitive sodium channels and that the high affinity binding sites are associated with a functional form of sodium channels. In contrast, Pidoplichko (29) has reported that two types of sodium currents recorded from ventricular cells can be distinguished by their sensitivity to TTX (K_D = 80 nM and 7 μM). Unequivocal answers to these molecular questions will require more detailed electrophysiological and biochemical experiments in smooth muscle. However, it is now clear that mammalian sodium channels are encoded by a multigene family and that separate genes encode for high and low affinity STX receptors (2, 30).

Recent publications have shown that, in isolated single smooth muscle cells, the dissociation constants of TTX against the sodium current range between 8 and 27 nM (8, 9). These concentrations are similar to the IC_{50} for TTX obtained in this study (8.8 nM), suggesting that the inhibitory effects of TTX may depend on an interaction with the high affinity binding sites for neurotoxins.

These results are the first direct demonstration of the existence of both high and low affinity binding sites for STX and TTX in myometrial smooth muscle cells. Conclusions from the electrophysiological results are in good agreement with those from biochemical studies. They suggest that binding of the neurotoxins to the high affinity sites may be involved in the inhibitory effects of STX and TTX on sodium channels, whereas low affinity binding sites may be associated with a nonfunctional subtype of sodium channels.

Acknowledgments

We thank Ms. N. Biendon for her excellent secretarial assistance.

References

1. Catterall, W. A. Neurotoxins that act on voltage-sensitive sodium channels in excitable membranes. *Annu. Rev. Pharmacol. Toxicol.* **20**:15–43 (1980).
2. Rogart, R. B., L. L. Cribbs, L. K. Muglia, D. D. Kephart, and M. W. Kaiser. Molecular cloning of a putative tetrodotoxin-resistant rat heart Na^+ channel isoform. *Proc. Natl. Acad. Sci. USA* **86**:8170–8174 (1989).
3. Benoît, E., A. Corbier, and J. M. Dubois. Evidence for two transient sodium currents in the frog node of Ranvier. *J. Physiol. (Lond.)* **361**:339–360 (1985).
4. Paponne, P. Voltage-clamp experiments in normal and denervated mammalian skeletal muscle fibres. *J. Physiol. (Lond.)* **306**:377–410 (1980).
5. Renaud, J. F., T. Kazazoglou, A. Lombet, R. Chicheportiche, E. Jaimovich, G. Romey, and M. Lazdunski. The Na^+ channel in mammalian cardiac cells. *J. Biol. Chem.* **258**:8799–8805 (1983).
6. Guo, X., A. Uehara, A. Ravindran, S. H. Bryant, S. Hall, and E. Moczydlowski. Kinetic basis for insensitivity to tetrodotoxin and saxitoxin in sodium channels of canine heart and denervated rat skeletal muscle. *Biochemistry* **26**:7546–7556 (1987).
7. Amédée, T., J. F. Renaud, K. Jmari, A. Lombet, J. Mironneau, and M. Lazdunski. The presence of Na^+ channels in myometrial smooth muscle cells is revealed by specific neurotoxins. *Biochem. Biophys. Res. Commun.* **137**:675–681 (1986).
8. Okabe, K., K. Kitamura, and H. Kuriyama. The existence of a highly tetrodotoxin sensitive Na channel in freshly dispersed smooth muscle cells of the rabbit main pulmonary artery. *Pflügers Arch.* **411**:423–428 (1988).
9. Ohya, Y., and N. Sperelakis. Fast Na^+ and slow Ca^{2+} channels in single uterine muscle cells from pregnant rats. *Am. J. Physiol.* **257**:C408–C412 (1989).
10. Dacquet, C., P. Pacaud, G. Loirand, C. Mironneau, and J. Mironneau. Comparison of binding affinities and calcium current inhibitory effects of a 1,4-dihydropyridine derivative (PN 200-110) in vascular smooth muscle. *Biochem. Biophys. Res. Commun.* **152**:1165–1172 (1988).
11. Bradford, M. M. A rapid and sensitive method for the quantitation of microgram quantities of protein utilizing the principle of protein-dye binding. *Anal. Biochem.* **72**:248–253 (1976).
12. Amédée, T., C. Mironneau, and J. Mironneau. Isolation and contractile responses of single pregnant rat myometrial cells in short-term primary culture and the effects of pharmacological and electrical stimuli. *Br. J. Pharmacol.* **88**:873–880 (1986).
13. Munson, P. J., and D. Rodbard. LIGAND: a versatile computerized approach for characterization of ligand binding systems. *Anal. Biochem.* **107**:220–239 (1980).
14. Honoré, E., T. Amédée, C. Martin, C. Dacquet, C. Mironneau, and J. Mironneau. Calcium channel current and its sensitivity to (+)isradipine in cultured pregnant rat myometrial cells. *Pflügers Arch.* **414**:477–483 (1989).
15. Cheng, Y. C., and W. H. Prussoff. Relationship between the inhibition constant (K_i) and the concentration of inhibitor which causes a 50 percent inhibition (I_{50}) of an enzymatic reaction. *Biochem. Pharmacol.* **22**:3099–3108 (1973).
16. Lindeman, B. Fluctuation analysis of sodium channels in epithelia. *Annu. Rev. Physiol.* **46**:497–515 (1984).
17. Sutro, J. B. Kinetics of veratridine action on Na channels of skeletal muscle. *J. Gen. Physiol.* **87**:1–24 (1986).
18. Barnes, S., and B. Hille. Veratridine modifies open sodium channels. *J. Gen. Physiol.* **91**:421–443 (1988).
19. Rando, T. A. Rapid and slow gating of veratridine-modified sodium channels in frog myelinated nerve. *J. Gen. Physiol.* **93**:43–65 (1989).
20. Lonnendonker, U. Binding of tetrodotoxin and saxitoxin to Na^+ channels at different holding potentials: fluctuation measurements in frog myelinated nerve. *Biochim. Biophys. Acta* **985**:161–167 (1989).
21. Moczydlowski, E., J. Mahar, and A. Ravindran. Multiple saxitoxin-binding sites in bullfrog muscle: tetrodotoxin-sensitive sodium channels and tetrodotoxin-insensitive sites of unknown function. *Mol. Pharmacol.* **33**:202–211 (1988).
22. Weigele, J. B., and R. L. Barchi. Analysis of saxitoxin binding in isolated rat synaptosomes using a rapid filtration assay. *FEBS Lett.* **91**:310–314 (1978).
23. Pauron, D., J. Barhanin, M. Amichot, M. Pralavorio, J. B. Berge, and M. Lazdunski. Pyrethroid receptor in the insect Na^+ channel: alteration of its properties in pyrethroid-resistant flies. *Biochemistry* **28**:1673–1677 (1989).
24. Catterall, W. A. Genetic analysis of ion channels in vertebrates. *Annu. Rev. Physiol.* **50**:395–406 (1988).
25. Wu, C. H., and T. Narahashi. Mechanisms of action of novel marine neurotoxins on ion channels. *Annu. Rev. Pharmacol. Toxicol.* **28**:141–161 (1988).
26. Lazdunski, M., and J. F. Renaud. The action of cardiotoxins on cardiac plasma membranes. *Annu. Rev. Physiol.* **44**:463–473 (1982).
27. Romey, G., and M. Lazdunski. Lipid-soluble toxins thought to be specific for Na^+ channels block Ca^{2+} channels in neuronal cells. *Nature (Lond.)* **297**:79–80 (1982).
28. Ulbricht, W. Rate of veratridine action on the nodal membrane. I. Fast phase determined during sustained depolarization in the voltage clamp. *Pflügers Arch.* **336**:187–199 (1972).
29. Pidoplichko, V. I. Two different tetrodotoxin-separable inward sodium currents in the membrane of isolated cardiomyocytes. *Gen. Physiol. Biophys.* **6**:593–604 (1986).
30. Noda, M., T. Ikeda, T. Kayane, H. Suzuki, H. Takeshima, M. Kurisaki, and S. Numa. Existence of distinct sodium channel messenger RNAs in rat brain. *Nature (Lond.)* **320**:188–192 (1986).

Send reprint requests to: Jean Mironneau, Laboratoire de Physiologie Cellulaire et Pharmacologie Moléculaire, INSERM JF 88-13, 3 place de la Victoire, 33076 Bordeaux Cédex, France.